Controlled exposure of CuO thin films through corrosion-protecting, ALD-deposited TiO 2 overlayers

Article *in* Zeitschrift fur Naturforschung B · September 2021

DOI: 10.1515/znb-2021-0117

5 authors, including:

Hamed Mehrabi
University of Arkansas
6 PUBLICATIONS **27** CITATIONS

SEE PROFILE

Hamed Mehrabi, Caroline G. Eddy,[#] Thomas I. Hollis,[#] Jalyn Vance,[#] and Robert H. Coridan*

Controlled exposure of CuO thin films through corrosion-protecting, ALD-deposited TiO_2 overlayers

https://doi.org/10.1515/znb-2021-0117

Received August 18, 2021; accepted August 23, 2021

***Corresponding author: Robert H. Coridan,** Materials Science and Engineering Program, University of Arkansas, Fayetteville, AR 72701, USA, and Department of Chemistry and Biochemistry, University of Arkansas, Fayetteville, AR 72701, USA; e-mail: rcoridan@uark.edu

Hamed Mehrabi: Materials Science and Engineering Program, University of Arkansas, Fayetteville, AR 72701, USA

Caroline G. Eddy, Thomas I. Hollis, Jalyn Vance: Department of Chemistry and Biochemistry, University of Arkansas, Fayetteville, AR 72701, USA

# These authors contributed equally to this work

Dedicated to Professor Richard Dronskowski on the Occasion of his 60th Birthday

Abstract: Ultra-thin film coatings are used to protect semiconductor photoelectrodes from the harsh chemical environments common to photoelectrochemical energy conversion. These layers add contact transfer resistance to the interface that can result in a reduction of photoelectrochemical energy conversion efficiency of the photoelectrode. Here, we describe the concept of a *partial* protection layer, which allows for direct chemical access to a small fraction of the semiconductor underlayer for further functionalization by an electrocatalyst. The rest of the interface remains protected by a stable, inert protection layer. CuO is used as a model system for this scheme. Atomic layer deposition (ALD)-prepared TiO_2 layers on CuO thin films prepared from electrodeposited Cu_2O allow for the control of interfacial morphology to intentionally expose the CuO underlayer. The ALD-TiO_2 overlayer shrinks during crystallization, while Cu_2O in the underlayer expands during oxidation. As a result, the TiO_2 protection layer cracks to expose the oxidized underlying CuO layer, which can be controlled by preceding thermal oxidation. This work demonstrates a potentially promising strategy for the parallel optimization of photoelectrochemical interfaces for chemical stability and high performance.

Keywords: protection layers, atomic layer deposition, cupric oxide, titanium dioxide, electrodeposition

1 Introduction

Photoelectrochemical (PEC) energy conversion is the process by which light energy is converted into chemical energy at a semiconductor-electrolyte interface. Photoelectrodes for these applications are designed with specific reactions and electrolyte conditions in mind, such as the hydrogen evolution (HER) or oxygen

evolution (OER) reactions that combine for the full water splitting reaction. Semiconductors with appropriate band edge energies for the target reaction may not be stable under otherwise desirable electrolyte conditions (1 M HCl or 1 M KOH, for example) or corrode under photoelectrochemical bias [1]. One solution to this problem has been the development of ultra-thin film protection layers (< 200 nm). A protection layer prevents direct contact between the semiconductor and the electrolyte while maintaining relative optical and electronic transparency. Atomic layer deposition (ALD) is a particularly useful method for preparing pinhole-free protection layers with precise thickness and composition [2]. A common material for these protection layers is amorphous TiO_2, which has a wide bandgap (>3.2 eV) and allows a relatively simple ALD deposition from water and organometallic precursors at temperatures below 200 C. TiO_2 layers are stable in many electrolytes, including extremely acidic or alkaline aqueous solutions. TiO_2 is intrinsically n-type which allows for electron conduction. However, the amorphous nature of the low temperature ALD-prepared TiO_2 may generate defect states that allow for hole transport through the layer as well [3]. ALD-TiO_2 protection layers have been used to stabilize a number of relevant semiconductor-electrolyte interfaces as they support charge transfer to electrocatalyst coatings [4–10]. Protection layers are not a panacea for perfecting PEC materials, however. The layer itself adds an additional interface and related resistances that are detrimental to device performance. Each additional layer may present a new set of limitations for further processing or functionalization. For example, the amorphous phase of TiO_2 crystallizes at temperatures that may be necessary for the chemical transformation of other functional components (oxidation or reduction of electrocatalysts layers). ALD-derived,

Al-doped ZnO (Al:ZnO) is included to improve interfacial resistances in TiO_2 protection layers but loses conductivity at relatively low annealing temperatures [8, 11, 12]. This suggests that it would be advantageous to develop strategies for partial protection layers, where the light absorber under the protection layer is partially exposed, allowing for further direct functionalization. An electrocatalyst can be added in direct electrical contact between the electrolyte and the light absorber layer through partially exposed regions. The rest of the material is protected by an inert overlayer rather than depending on carrier conductivity properties of the protection layer.

Here, we explore the partial protection of a CuO thin film as a model system for partial protection layer strategies. CuO is of interest as a hydrogen-evolving photocathode for solar-driven water splitting because it is composed of earth-abundant materials and has a relatively small band gap compared to other metal oxides (1.3 eV) [13]. It can be prepared by air annealing electrodeposited Cu_2O thin films. CuO is unstable under most electrolyte conditions relevant to PEC water splitting and needs an additional co-electrocatalyst (Pt, for example) to produce hydrogen under illumination. A conformal layer of Pt could protect the CuO layer from dissolution but will generate parasitic absorption and potentially disrupt the photovoltage-generating semiconductor-liquid junction [14]. As has been shown to be the case for Cu_2O, an ALD-derived full protection layer requires both Al:ZnO and TiO_2, which allows for high short-circuit photocurrents but results in a loss of a significant fraction of the possible open-circuit photovoltage compared to a plain, unprotected photocathode [11]. A CuO-based photocathode can potentially benefit from partial protection that appropriately balances direct light-absorber/electrocatalyst contact and the chemical stability of the interface.

More fundamentally, the combination of materials offers insight into the formation of three-dimensional composites from a one-dimensional, intentionally layered heterostructure. When annealed in air, Cu_2O transforms into CuO (a 5.9% volume increase per Cu atom based on the densities of each compound) while amorphous, ALD-derived TiO_2 (denoted ALD-TiO_2) contracts by roughly 7% upon annealing [15]. This raises the question of how the morphology of the layered Cu_2O/ALD-TiO_2 heterostructure transforms under these opposing mechanical strains and whether that may result in a useful strategy for the partial protection of CuO. Herein, we describe the resulting morphological transformation of air-annealed heterostructures of electrodeposited Cu_2O coated by ALD-TiO_2. We find that air-annealing results in the individual transformation of each layer (Cu_2O to CuO and amorphous TiO_2 to anatase) rather than the formation of a ternary compound such as $CuTiO_3$. The contraction of the TiO_2 layer displays a morphological transformation similar to desiccation crack formation in drying mud [16, 17]. The CuO expands through these cracks, becoming partially exposed to the electrolyte interface. These results suggest that the exploitation of dissimilar mechanical behaviors under annealing conditions is a strategy for the partial protection in this combination of materials.

2 Materials and methods

Water (HPLC grade, VWR), acetone (99.5%, EMD Millipore Corp), methanol (HPLC grade, Merck) and isopropanol (HPLC grade, Merck) were used as received. Copper sulfate pentahydrate (>98.0%, Sigma-Aldrich), lactic acid (reagent grade, >85%, Sigma-Aldrich) and NaOH (50% (*w*/*w*), VWR) were used as received. Fluorine-doped tin oxide (FTO)-coated substrates (TEC-15 glass, 12–14 Ω sq, MTI Corp.) were cut to roughly 1

cm x 2 cm pieces, rinsed sequentially in acetone, methanol, isopropanol, and water, then dried under nitrogen before electrodeposition.

Powder X-ray diffraction (XRD) measurements were performed using a Rigaku Mini-Flex II Diffractometer with Cu*Kα* radiation (λ = 1.54 Å). Scanning electron microscopy (SEM) was performed with a FEI Nova Nanolab SEM equipped with a Bruker Quantax Energy-dispersive X-ray Spectrometer (EDX). X-ray photoemission spectroscopy (XPS) measurements were performed with a Phi Versaprobe XPS instrument using a monochromated Al*Kα* source (E = 1486.6 eV). The X-ray spot size was 100 μm x 100 μm for each XPS measurement. All absolute energies for XPS measurements were calibrated to the adventitious carbon feature at 284.8 eV from C 1s spectra measured for each sample [18].

2.1 Electrodeposition of Cu_2O

Cuprous oxide was electrodeposited on FTO electrodes by methods described in detail elsewhere [19, 20]. The electrodeposition bath was initially prepared as a 40. mM solution of $CuSO_4 \bullet 5H_2O$ in 3 M aqueous lactic acid. NaOH was slowly titrated into the solution to increase the pH to 10.0. Cu_2O films were prepared by potentiostatic electrodeposition (Bio-Logic SP-50) in a three-neck flask submerged in a water bath to maintain the electrodeposition bath temperature at 45 C. The FTO glass working electrode was held at –0.4 V vs. an Ag/AgCl reference electrode (saturated KCl; BASi, Inc.) with a Cu wire counter electrode. The thickness of the Cu_2O layer was controlled by the duration of the electrodeposition, which was 15 minutes unless otherwise noted. CuO was prepared by annealing electrodeposited Cu_2O in air in a muffle furnace at 500 C for the noted time (3 K min^{-1} ramp rate).

2.2 Atomic layer deposition of TiO_2

Thin films of ALD-TiO_2 were deposited onto electrodeposited Cu_2O and CuO thin films by atomic layer deposition in a commercial ALD reactor (Gemstar XT-6; Arradiance). The reaction chamber was heated to 150 C under a constant 20 sccm flow of ultra-high purity N_2 (99.999%; AirGas). The ALD-TiO_2 was deposited from the sequential exposure of the substrates to vapors of tetrakis(dimethylamido)titanium (TDMAT; 98%, Strem) and water. The TDMAT precursor bottle was heated to 78 C to provide sufficient vapor pressure for the deposition. The ALD deposition was performed by repeating the following sequence for the desired number of exposures: 100 ms TDMAT pulse, 25 s reactor purge, 15 ms water pulse, 25 s reactor purge. Electrodes were rinsed with water before being inserted into the reactor chamber. All post-ALD deposition annealing steps were performed by heating the samples in air in a muffle furnace at 500 C for 1 hour (3 K min^{-1} ramp rate).

3 Results and Discussion

Air oxidation of ALD-TiO_2 layers is not expected to form a stable ternary compound with CuO as other metal oxides do ($CuFeO_2$, $CuWO_4$, $CuBi_2O_4$, and others) [21–27]. CuO and TiO_2 have a eutectic point at temperatures greater than 900 C, which can then be quenched to form metastable Cu-Ti-O compounds [28, 29]. We were not able to find similar characterization for the composite product(s) formed from the thermal oxidation of Cu_2O and TiO_2. Figure 1 shows the results of powder diffraction measurements of Cu_2O electrodes coated with 1500 cycles (60 nm) of ALD TiO_2 before and after annealing in air for 1 h at 500 C. No crystalline phases of TiO_2 were observed, and Cu_2O (ICDD PDF 01-071-4310) was the only form of copper oxide present before

annealing. This was consistent with the expectation of a layered Cu_2O-amorphous ALD-TiO_2 heterostructure. After annealing, the Cu_2O was oxidized completely to CuO (ICDD PDF 00-044-0706), and the ALD-TiO_2 crystallized to anatase TiO_2 (ICDD PDF 00-001-5062), as indicated by the appearance of intensity at 25.2º, which corresponds to the (101) anatase Bragg reflection. No peaks indicating the formation of ternary compounds were observed, nor was the Cu_2O protected from oxidation at this relatively modest temperature. For comparison, a CuO electrode was coated with 1500 cycles of ALD-TiO_2 and annealed in air. Prior to the annealing, CuO was the only crystalline phase observed other than the substrate. After the annealing step, anatase TiO_2 was visible in the diffractogram.

We used XPS to track the interfacial migration of the layers due to the annealing process (Figure 2). The XPS Ti 2p intensity was consistent across the surface and on multiple samples before annealing, but after the annealing step, the feature varied in intensity across the surface of the same electrode. We also observed CuO at the surface. Based on the powder diffraction results (Figure 1), the surface was a CuO-TiO_2 composite. SEM imaging before (Figure 3a,b) and after (Figure 3c,d) the annealing step showed that the CuO emerges from cracks in the anatase TiO_2 layer. The CuO emerges through the separation between crystalline TiO_2 domains, which forms when the layer shrinks. The morphology of the extruded layer of CuO is generated by the noted volume increase in the layer as the precursor Cu_2O is oxidized. While the ALD-TiO_2 layer remained at the interface as a partial protection layer, the morphology of the extruded CuO caused significant exposure of the underlayer to the interface. Driving CuO to the surface through the extreme volume change that occurs for the oxidation of

Cu_2O is not likely an effective strategy for synthesizing a partial protection layer for the CuO light absorber.

A thinner ALD-TiO_2 layer showed a more dramatic exchange of CuO for TiO_2 at the interface (Figure 4). When the Cu_2O was coated with a relatively thin ALD-TiO_2 layer (300 cycles, or 12 nm), only the XPS signal of Ti (IV) was observed [30]. This indicated that the overlayer was thick enough to prevent the detection of the underlying Cu_2O via XPS. After annealing, we observed an interface devoid of any TiO_2 and entirely composed of CuO. The TiO_2 was no longer observed in the XPS measurements. EDX spectra of the heterostructure showed that the quantity of Cu and Ti in the film was effectively identical before and after the annealing step (Figure 5). This is consistent with the migration of CuO to the surface, driven by expansion during oxidation. These results suggest that the TiO_2 layer becomes enshrouded by the expanding CuO forming underneath. The TiO_2 is hidden from the surface and no longer serves as a protection layer.

Annealing the Cu_2O to form CuO prior to the ALD-TiO_2 deposition resulted in more conservative control over the morphological transformation of the interface. The powder diffractograms of a CuO film (prepared by annealing Cu_2O for 3 h) coated with 1500 cycles of ALD-TiO_2 before and after air annealing are shown in Figure 1. The CuO remained unchanged while the ALD-TiO_2 crystallized to anatase during the annealing. On some portions of the heterostructure, the desiccation-like cracks had formed in the TiO_2 overlayer after annealing with minor extrusion of the CuO from underneath (Figure 6a). In some regions of the heterostructure, cracks did not form (Figure 6b). Point EDX spectra (Figure 6c) showed a more intense Cu signal and reduction in the Sn signal on

the ‘ridge’ versus the planar ‘plateau’ in the region from Figure 6a. The amount of TiO_2 was the same in both spectra. This indicates that the CuO was thicker in this region and had physically extruded through the TiO_2 overlayer. The CuO in the underlayer does not expand due to oxidation as the Cu_2O films do. We hypothesize that cracks form where some remaining interfacial Cu_2O is present to drive the crack formation rather than solely relying on the contraction of the TiO_2 overlayer.

To test this hypothesis, we reduced the duration of the Cu_2O-to-CuO annealing step to 1 h to increase the amount of residual Cu_2O. We observed that the TiO_2 layer uniformly generated the desiccation-like cracking throughout the entire film (Figure 7a). Additionally, we observed the growth of blooms of material extruding through the surface layer (Figure 7b,c). The EDX spectrum (Figure 8) of the material in the bloom region (green cross in Fig 7b) shows roughly four times the Cu compared to the EDX in the plateau (magenta cross in Fig. 7b). The Sn signal is negligible in the bloom region spectrum, which indicates that the blooms are a significant Cu-containing growth that is so thick that it obscures the FTO substrate. These bloom points are another accessible functionalization target for directly addressing the CuO layer underneath the TiO_2 layer. The magnitude of desiccation-like cracking was significantly reduced for CuO layers that were annealed for longer times. Figure 8 shows the interface for a heterostructure where the CuO underlayer was prepared by annealing Cu_2O in air for 24 h prior to the deposition of 1500 cycles of ALD-TiO_2. The complete heterostructure was then annealed for 1 h, consistent with the other samples reported here. Some slight desiccation-like cracking was observed, though the characteristic size of the plateau regions (> 4–5 μm diameter) was increased compared to CuO formed from 1 h (Figure

7) and 3 h (Figure 6) oxidation steps (< 2 μm diameter). The crack formation was relatively uniform across the entire interface, and no blooming was observed on the surface of the material. This suggests that the mechanical forces driving the cracking and extrusion process had been diminished by increasing the oxidation time for the CuO base layer and a reduction in the amount of residual Cu_2O. This is consistent with our hypothesis that the expansion of residual Cu_2O in the base layer affects the formation of cracks and the degree of exposure through the ALD-TiO_2 protection layer. Here, we have shown that the morphology and composition of the interface of a CuO-TiO_2 heterostructure can be controlled by the thermal annealing process both during the CuO formation from Cu_2O and in post-ALD processing. The rationale for controlling this structure is to provide partial access to the base CuO layer while maintaining significant surface coverage from the ALD-TiO_2 overlayer. The exposure of the underlying CuO provides a route for further functionalization while maintaining a significant fraction of TiO_2-protected surface area. For example, the TiO_2 protection layer can act as a blocking layer for electrodeposition or electroless deposition of Pt or other electrocatalyst materials. The added electrocatalyst can potentially make direct contact to the functional CuO light absorber while being limited to minimize coverage. This partial protection scheme balances the formation of direct semiconductor-electrocatalyst interfaces with protection that avoids the parasitic absorption and deleterious effects to the photovoltage-generating barrier height of the semiconductor-electrolyte contact [14]. The specific approach to the CuO-TiO_2 composite takes advantage of their inability to form a single, ternary compound under the relatively low temperatures studied here. More general approaches to partial protection schemes will require the identification of

other routes to develop structural exposure such as area-selective ALD processing [31–33].

4 Conclusion

In summary, we have studied the structural transformations of layered copper oxide/ALD-TiO_2 heterostructures under oxidative annealing. The interfacial structure and morphology of the post-annealed structure can be controlled by the choice of solid-state precursors prior to annealing. The ALD-TiO_2 overlayer forms cracks due to the oxidative contraction from an amorphous oxide to the anatase phase. An initial Cu_2O layer is oxidized to CuO, which causes the underlayer to expand and extrude to the surface through the cracks in thick anatase TiO_2. For thin overlayers, the extrusion of CuO results in an enveloped TiO_2 layer, hiding it from the interface. Thermal control over structure and morphology of the interface can potentially be useful for photoelectrochemical applications. Of note, we posed the strategy of a partial protection layer, where annealing yields a small exposure of the light-absorber underlayer to further functionalization.

Acknowledgements: This manuscript was prepared in dedication to Prof. Dr. Richard Dronskowski in honor of his 60th birthday. This material is based upon work supported by the U.S. Department of Energy, Office of Science, Office of Basic Energy Sciences under Award Number DE-SC-0020301.

1. Chen, S., Wang, L.-W. Thermodynamic Oxidation and Reduction Potentials of Photocatalytic Semiconductors in Aqueous Solution. *Chem. Mater*. 2012, *24*, 3659–3666. https://doi.org/10.1021/cm302533s
2. George, S. M. Atomic Layer Deposition: An Overview. *Chem. Rev*. 2010, *110*, 111–131. https://doi.org/10.1021/cr900056b

3. Hu, S., Shaner, M. R., Beardslee, J. A., Lichterman, M., Brunschwig, B. S., Lewis, N. S. Amorphous TiO_2 coatings stabilize Si, GaAs, and GaP photoanodes for efficient water oxidation. *Science* 2014, *344*, 1005–1009. https://doi.org/10.1126/science.1251428

4. McDowell, M. T., Lichterman, M. F., Spurgeon, J. M., Hu, S., Sharp, I. D., Brunschwig, B. S., Lewis, N. S. Improved Stability of Polycrystalline Bismuth Vanadate Photoanodes by Use of Dual-Layer Thin TiO_2/Ni Coatings. *J. Phys. Chem. C* 2014, *118*, 19618–19624 (). https://doi.org/10.1021/jp506133y

5. Hu, S., Lewis, N. S., Ager, J. W., Yang, J., McKone, J. R., Strandwitz, N. C. Thin-Film Materials for the Protection of Semiconducting Photoelectrodes in Solar-Fuel Generators. *J. Phys. Chem. C* 2015, *119*, 24201–24228. https://doi.org/10.1021/acs.jpcc.5b05976

6. Sun, K., Liu, R., Chen, Y., Verlage, E., Lewis, N. S., Xiang, C. A Stabilized, Intrinsically Safe, 10% Efficient, Solar-Driven Water-Splitting Cell Incorporating Earth-Abundant Electrocatalysts with Steady-State pH Gradients and Product Separation Enabled by a Bipolar Membrane. *Adv. Energy Mater*. 2016, *6*, 1600379. https://doi.org/10.1002/aenm.201600379

7. Bronneberg, A. C., Höhn, C., van de Krol, R. Probing the Interfacial Chemistry of Ultrathin ALD-Grown TiO_2 Films: An In-Line XPS Study. *J. Phys. Chem. C* 2017, *121*, 5531–5538. https://doi.org/10.1021/acs.jpcc.6b09468

8. Reed, P. J., Mehrabi, H., Schichtl, Z. G., Coridan, R. H. Enhanced Electrochemical Stability of TiO_2-Protected, Al-doped ZnO Transparent Conducting Oxide Synthesized by Atomic Layer Deposition. *ACS Appl. Mater. Interfaces* 2018, *10*, 43691–43698. https://doi.org/10.1021/acsami.8b16531

9. Ma, Z., Thersleff, T., Görne, A. L., Cordes, N., Liu, Y., Jakobi, S., Rokicinska, A., Schichtl, Z. G., Coridan, R. H., Kustrowski, P., Schnick, W., Dronskowski, R., Slabon, A. Quaternary Core–Shell Oxynitride Nanowire Photoanode Containing a Hole-Extraction Gradient for Photoelectrochemical Water Oxidation. *ACS Appl. Mater. Interfaces* 2019, *11*, 19077–19086. https://doi.org/10.1021/acsami.9b02483

10. Dias, V. M., Chiappim, W., Fraga, M. A., Maciel, H. S., Marciano, F. R., Pessoa, R. S. Atomic layer deposition of TiO_2 and Al_2O_3 thin films for the electrochemical study of corrosion protection in aluminum alloy cans used in beverage. *Mater. Res. Express* 2020, *7*, 076408. https://doi.org/10.1088/2053-1591/aba557

11. Paracchino, A., Laporte, V., Sivula, K., Grätzel, M., Thimsen, E. Highly active oxide photocathode for photoelectrochemical water reduction. *Nat Mater*. 2011, *10*, 456–461. https://doi.org/10.1038/nmat3017

12. Paracchino, A., Mathews, N., Hisatomi, T., Stefik, M., Tilley, S. D., Grätzel, M. Ultrathin films on copper(I) oxide water splitting photocathodes: a study on performance and stability. *Energy Environ. Sci*. 2012, 5, 8673–8681. https://doi.org/10.1039/C2EE22063F

13. Jayatissa, A. H., Guo, K., Jayasuriya, A. C. Fabrication of cuprous and cupric oxide thin films by heat treatment. *Appl. Surf. Sci*. 2009, *255*, 9474–9479. https://doi.org/10.1016/j.apsusc.2009.07.072

14. Rossi, R. C., Lewis, N. S. Investigation of the Size-Scaling Behavior of Spatially Nonuniform Barrier Height Contacts to Semiconductor Surfaces Using Ordered Nanometer-Scale Nickel Arrays on Silicon Electrodes. *J. Phys. Chem. B* 2001, *105*, 12303–12318. https://doi.org/10.1021/jp011861c

15. Rich, B. B., Etinger-Geller, Y., Ciatto, G., Katsman, A., Pokroy, B. Retention of surface structure causes lower density in atomic layer deposition of amorphous titanium oxide thin films. *Phys. Chem. Chem. Phys*. 2021, *23*, 6600–6612. https://doi.org/10.1039/D1CP00341K

16. Peron, H., Laloui, L., Hu, L.-B., Hueckel, T. Formation of drying crack patterns in soils: a deterministic approach. *Acta Geotech*. 2013, *8*, 215–221. https://doi.org/10.1007/s11440-012-0184-5

17. Goehring, L., Morris, S. W. Cracking mud, freezing dirt, and breaking rocks. *Physics Today* 2014, *67*, 39–44. https://doi.org/10.1063/PT.3.2584

18. Barr, T. L., Seal, S. Nature of the use of adventitious carbon as a binding energy standard. *J. Vacuum Sci. & Technol. A* 1995, *13*, 1239–1246. https://doi.org/10.1116/1.579868

19. Golden, T. D., Shumsky, M. G., Zhou, Y., VanderWerf, R. A., Van Leeuwen, R. A., Switzer, J. A. Electrochemical Deposition of Copper(I) Oxide Films. *Chem. Mater*. 1996, *8*, 2499–2504. https://doi.org/10.1021/cm9602095

20. Lowe, J. M., Yan, Q., Benamara, M., Coridan, R. H. Direct photolithographic patterning of cuprous oxide thin films via photoelectrodeposition. *J. Mater. Chem. A* 2017, *5*, 21765–21772. https://doi.org/10.1039/C7TA05321E

21. Read, C. G., Park, Y., Choi, K.-S. Electrochemical Synthesis of p-Type $CuFeO_2$ Electrodes for Use in a Photoelectrochemical Cell. *J. Phys. Chem. Lett*. 2012, *3*, 1872–1876. https://doi.org/10.1021/jz300709t

22. John, M., Heuss-Aßbichler, S., Park, S.-H., Ullrich, A., Benka, G., Petersen, N., Rettenwander, D., Horn, S. R. Low-temperature synthesis of $CuFeO_2$ (delafossite) at 70°C: A new process solely by precipitation and ageing. *J. Solid State Chem*. 2016, *233*, 390–396. https://doi.org/10.1016/j.jssc.2015.11.011

23. Yourey, J. E., Bartlett, B .M. Electrochemical deposition and photoelectrochemistry of $CuWO_4$, a promising photoanode for water oxidation. *J. Mater. Chem*. 2011, *21*, 7651–7660. https://doi.org/10.1039/C1JM11259G

24. Chen, Z., Löber, M., Rokicińska, A., Ma, Z., Chen, J., Kuśtrowski, P., Meyer, H.-J., Dronskowski, R., Slabon, A. Increased photocurrent of $CuWO_4$ photoanodes by modification with the oxide carbodiimide $Sn_2O(NCN)$. *Dalton Trans*. 2020, *49*, 3450–3456. https://doi.org/10.1039/C9DT04752B

25. Ungelenk, J., Speldrich, M., Dronskowski, R., Feldmann, C. Polyol-mediated low-temperature synthesis of crystalline tungstate nanoparticles MWO_4 (M = Mn, Fe, Co, Ni, Cu, Zn). *Solid State Sci*. 2014, *31*, 62–69. https://doi.org/10.1016/j.solidstatesciences.2014.02.020

26. Weller, M. T., Lines, D. R. Structure and oxidation state relationships in ternary copper oxides. *J. Solid State Chem*. 1989, *82*, 21–29. https://doi.org/10.1016/0022-4596(89)90217-X

27. Rajeshwar, K., Hossain, M. K., Macaluso, R. T., Janáky, C., Varga, A., Kulesza, P. J. Review—Copper Oxide-Based Ternary and Quaternary Oxides: Where Solid-State Chemistry Meets Photoelectrochemistry. *J. Electrochem. Soc*. 2018, *165*, H3192–H3206. https://doi.org/10.1149/2.0271804jes

28. de la Rubia, M. A., Reinosa, J. J., Leret, P., Romero, J. J., de Frutos, J., Fernández, J. F. Experimental determination of the eutectic temperature in air of the $CuO–TiO_2$ pseudobinary system. *J. Eur. Ceram. Soc*. 2012, *32*, 71–76. https://doi.org/10.1016/j.jeurceramsoc.2011.07.026

29. Nie, J., Chan, J. M., Qin, M., Zhou, N., Luo, J. Liquid-like grain boundary complexion and sub-eutectic activated sintering in CuO-doped TiO_2. *Acta Mater*. 2017, *130*, 329–338. https://doi.org/10.1016/j.actamat.2017.03.037

30. Moulder, J. F., Stickle, W. F., Sobol, P. E., Bomben, K. D. Handbook of X Ray Photoelectron Spectroscopy: A Reference Book of Standard Spectra for Identification and Interpretation of Xps Data. Physical Electronics, Eden Prairie, Minn. (1995).

31. Chen, R., Kim, H., McIntyre, P. C., Porter, D. W., Bent, S. F. Achieving area-selective atomic layer deposition on patterned substrates by selective surface modification. *Appl. Phys. Lett*. 2005, *86*, 191910. https://doi.org/10.1063/1.1922076

32. Chen, R., Bent, S. F. Chemistry for Positive Pattern Transfer Using Area-Selective Atomic Layer Deposition. *Adv. Mater*. 2006, *18*, 1086–1090. https://doi.org/10.1002/adma.200502470

33. Fang, M., Ho, J. C. Area-Selective Atomic Layer Deposition: Conformal Coating, Subnanometer Thickness Control, and Smart Positioning. *ACS Nano* 2015, 150909103635004. https://doi.org/10.1021/acsnano.5b05249

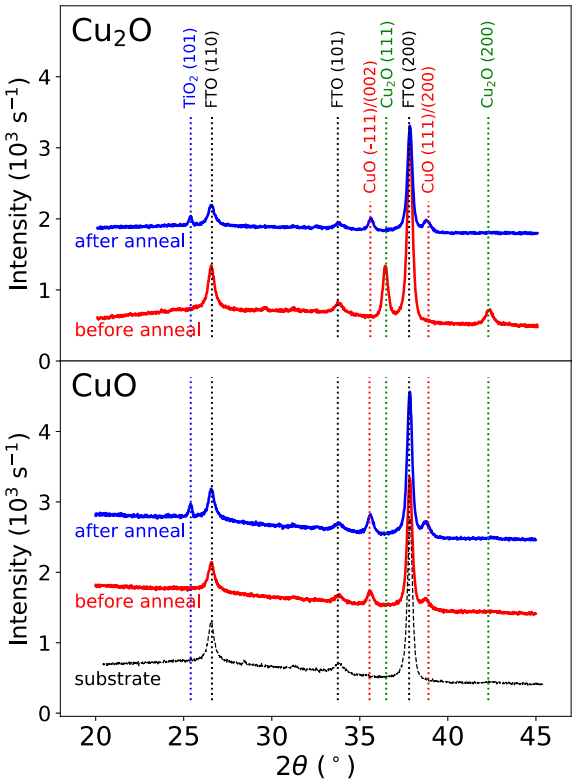

Fig. 1: X-ray diffraction measurements of layered copper oxide/ALD-TiO_2 heterostructures before (red) and after (blue) annealing in air at 500 ºC for 1 hr (3.0 K min^{-1} ramp). The Cu_2O samples were coated with 1500 cycles of ALD-TiO_2 before the annealing step, while the CuO samples were annealed to oxidize the precursor electrodeposited Cu_2O film before the ALD-TiO_2 layer was added. The FTO/glass substrate diffraction measurement (black) is included for comparison.

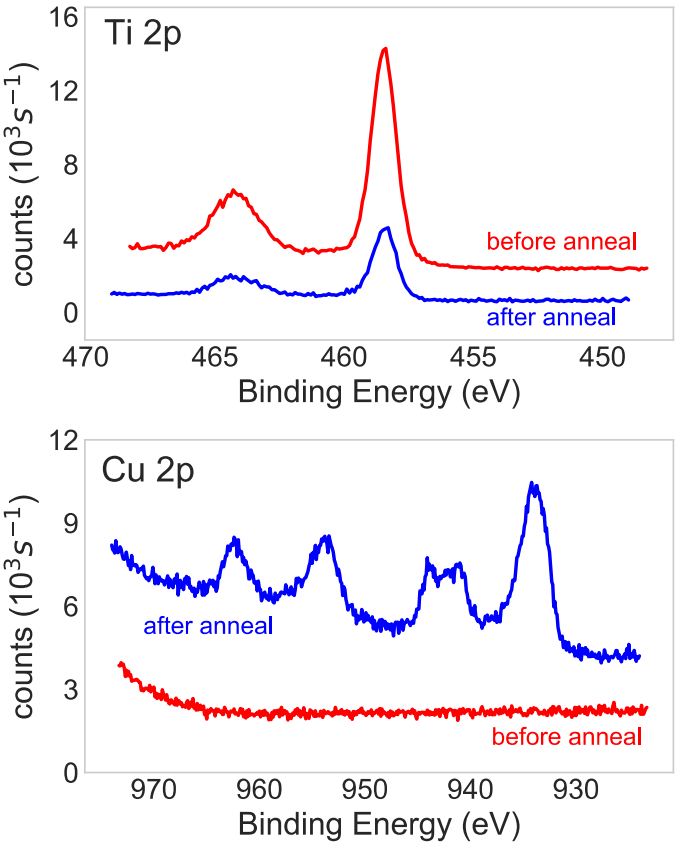
Ti 2p
counts ($10^3 s^{-1}$)
16
12
8
4
0
before anneal
after anneal
470
465
460
455
450
Binding Energy (eV)
Cu 2p
counts ($10^3 s^{-1}$)
12
9
6
3
0
after anneal
before anneal
970
960
950
940
930
Binding Energy (eV)

Fig. 2: Ti 2*p* and Cu 2*p* XPS spectra of a Cu_2O/ALD-TiO_2 layered heterostructure before (red) and after (blue) annealing in air. The ALD-TiO_2 layer was prepared by 1500 cycles of ALD (approximately 60 nm). The reduction of intensity in the Ti 2*p* XPS feature (characteristic of TiO_2) and the appearance of the Cu 2*p* feature (characteristic of CuO) after annealing indicates that CuO migrates to the surface of the heterostructure upon annealing.

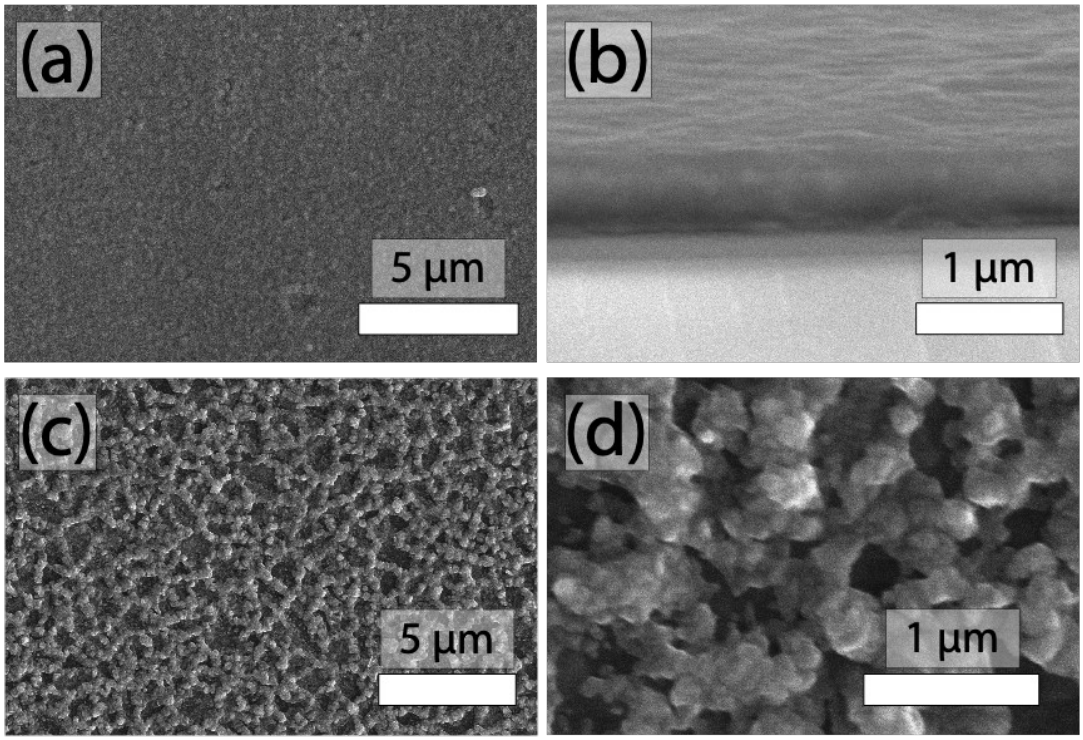

Fig. 3: (a) Surface morphology and (b) cross-sectional SEM of the Cu_2O/ALD-TiO_2 layered heterostructure from (Figure 2) before annealing. The 1500 cycle ALD-TiO_2 layer was roughly 60 nm and the Cu_2O layer was roughly 280 nm. (c) Surface morphology and (d) high-magnification SEM of the same heterostructure after annealing in air. The CuO extrudes through cracks in the ALD film.

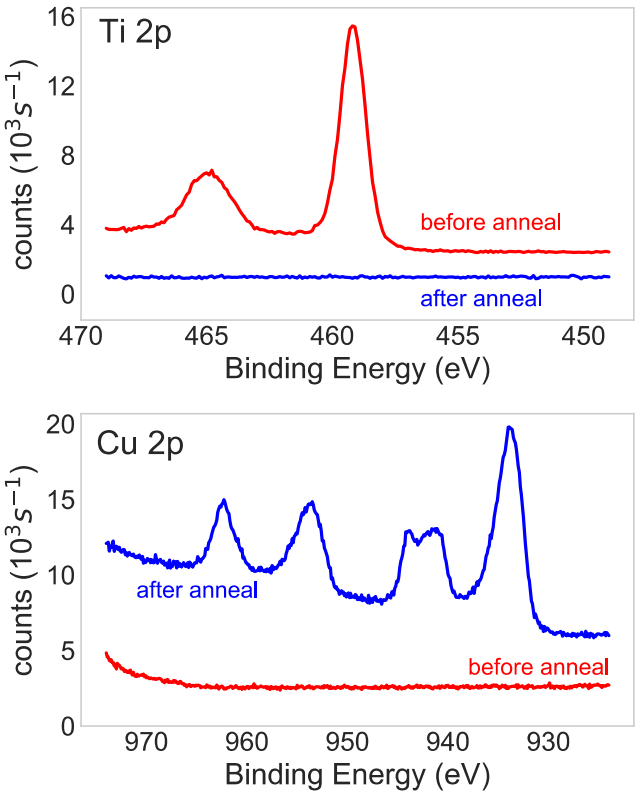

Fig. 4: Ti 2*p* and Cu 2*p* XPS spectra of a Cu_2O/ALD-TiO_2 layered heterostructure before (red) and after (blue) annealing in air. The ALD-TiO_2 layer was prepared by 300 cycles of ALD. Prior to annealing in air, the surface was entirely composed of the ALD-TiO_2 layer. After annealing, only the CuO XPS feature observed. The disappearance of the TiO_2 signal from the Ti 2*p* XPS measurement indicates that the CuO completely encapsulated the initial ALD-TiO_2 overlayer.

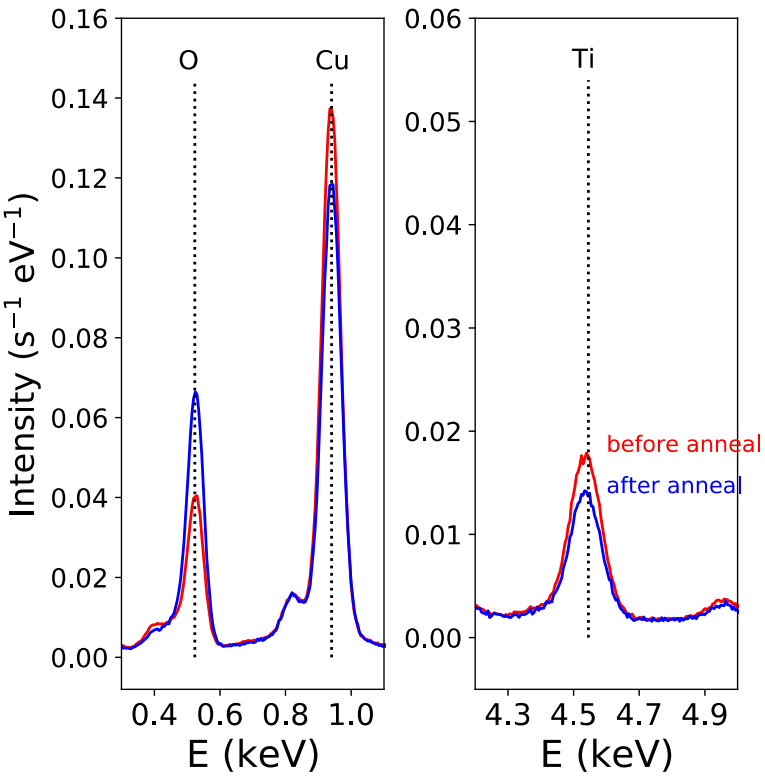

Fig. 5: EDX spectra of the Cu_2O/ALD-TiO_2 heterostructure formed with 300 cycles of ALD before (red) and after (blue) annealing. While XPS measurements showed that the CuO formed during annealing encapsulated the TiO_2 that resided on the top of the heterostructure before annealing. The EDX spectra showed that, while the interface had transformed, the Ti and Cu were still in the heterostructure in the same proportion. Variance in the two measurements was due to heterogeneity between film thicknesses on different locations on the sample.

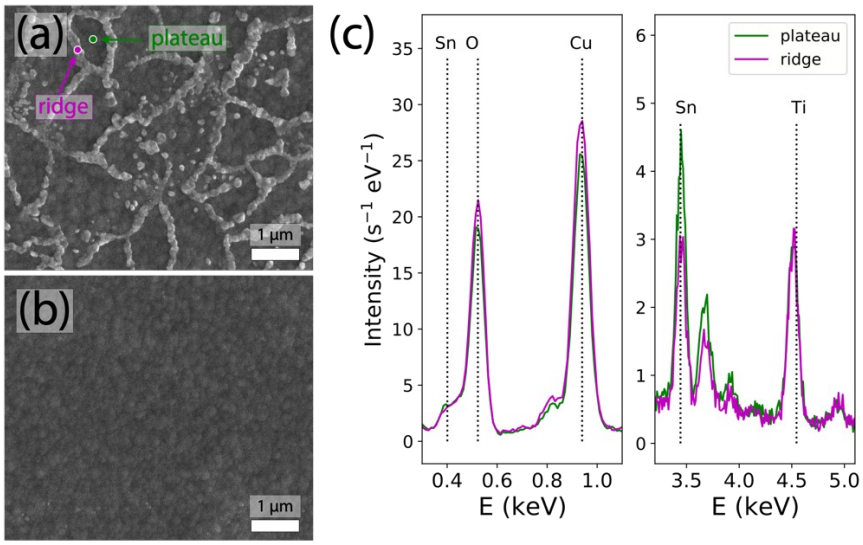

Fig. 6: (a) A portion of the CuO/ALD-TiO_2 (1500 cycles) where CuO (prepared by air oxidation of Cu_2O for 3 h at 500 ºC) partially extruded through cracks in the TiO_2 overlayer. (b) Other portions of the CuO/ALD-TiO_2 (1500 cycles) did not show extruded CuO while the TiO_2 crystallized, suggesting that the underlayer extrusion is partially driven by the expansion of the underlayer. (c) Point EDX spectra of the ridge (magenta) and plateau (green) regions denoted in (a). The Cu signal increased and the Sn signal decreased, while the Ti signal remained unchanged. This suggests that the ridge is thicker and contains more Cu than the TiO_2 protected region.

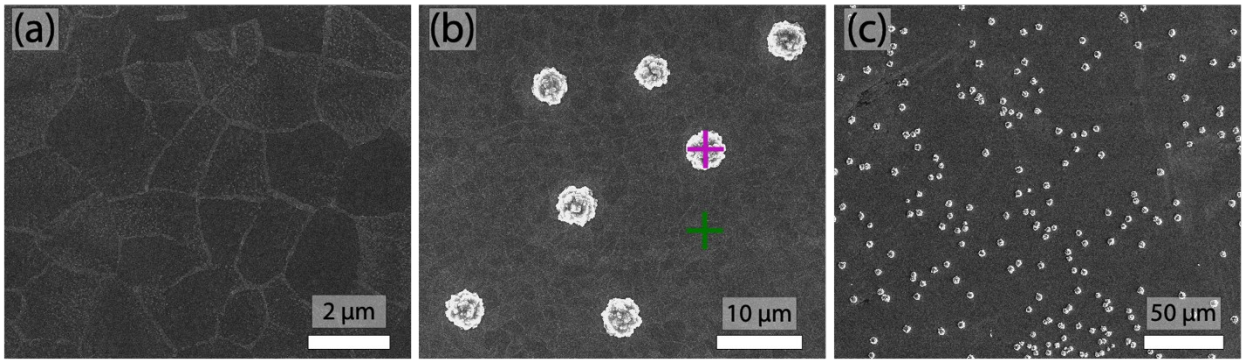

Fig. 7: (a) SEM images of desiccation crack formation on a CuO/ALD-TiO_2 (1500 cycles) film annealed for 1 h. The CuO was prepared by annealing Cu_2O annealed in air for 1 h before TiO_2 deposition. This degree of cracking was observed over the entire interface. (b) Extruded material 'blooms' (magenta cross) were observed on the 1 h CuO film that were not observed on the 3 h CuO film in Figure 6. EDX spectra for the 'bloom' and the plateau region (green cross) are shown in Figure 7. (c) The large scale 'blooms' were observed across the entire film.

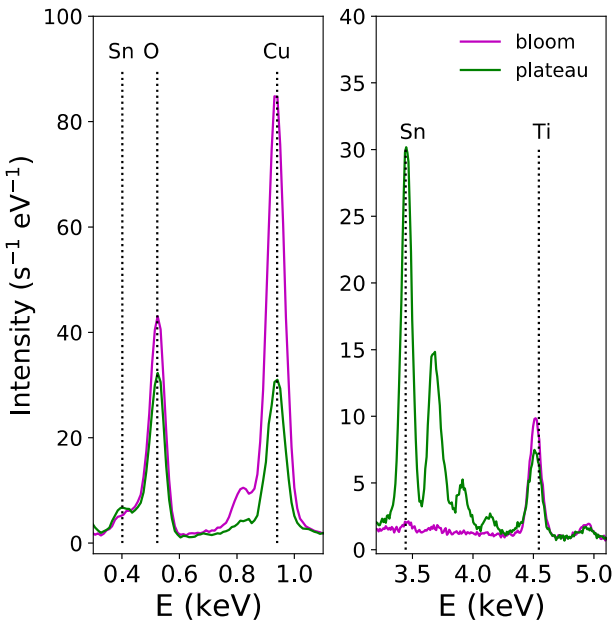

Fig. 8: EDX spectra of the material ‘bloom’ and ‘plateau’ regions from Figure 7b. The increased Cu EDX signal and the negligible Sn EDX signal in the ‘bloom’ spectrum (magenta) compared to the ‘plateau’ spectrum (green) indicates that the extruded material is Cu-rich and sufficiently thick to obscure the FTO substrate.

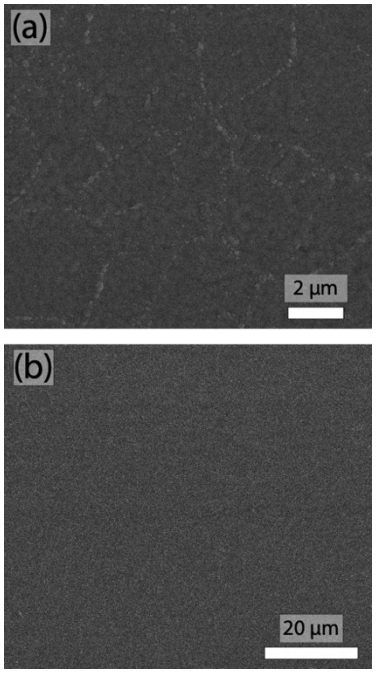

Fig. 9: (a) High-magnification and (b) low-magnification SEM images of the reduced desiccation cracking on CuO thin films prepared by annealing Cu_2O in air for 24 h before the deposition of 1500 cycles of ALD-TiO_2 and 1 h of annealing. Minimal extrusion of the CuO underlayer was observed compared to the 1 h (Figure 7) and 3 h (Figure 6).